

## 核设施退役 $\gamma$ 源项现场测量技术研究

肖雪夫 宋利军 王玉来 文富平 廖海涛  
班莹 夏益华 李瑞香 李航 涂兴民

(中国原子能科学研究院,北京,102413)

### 摘 要

非破坏性分析技术(NDA)是核设施退役特性调查中的重要技术之一。就地 $\gamma$ 谱仪是一类可专门用于核设施建筑物和现场清污测量、放射性污染源项调查的NDA装置,其探测器必须进行合适的校准。报告给出一种新的用于核设施退役中放射性非破坏性测量的就地HPGe $\gamma$ 谱仪探测器的校准技术,即蒙特卡罗方法模拟计算校准技术。采用校准了的一台就地HPGe $\gamma$ 谱仪对中国原子能科学研究院的核设施/实验室的不锈钢管和不锈钢罐进行了现场就地测量分析,同时取样进行实验室样品分析;还对核工业航测遥感中心的大体积辐射模型(铀、镭、钍)进行了就地测量分析。就地测量结果与实验室样品分析及大体积辐射模型标称值的相对偏差小于 $\pm 45.0\%$ 。

关键词: 刻度 MCNP 就地 HPGe  $\gamma$  谱仪 退役

# Study on a New Calibration Methods of in-situ HPGe $\gamma$ Spectrometers used for Non-destructive Analyzing Radioactivity in Nuclear Facilities Decommissioning

XIAO Xuefu SONG Lijun WANG Yulai WEN Fuping LIAO Haitao  
BAN Ying XIA Yihua LI Ruixiang LI Hang TU Xingmin  
(China Institute of Atomic Energy, Beijing, 102413)

## ABSTRACT

A new calibration technique, which is the Monte Carlo modeling technique, of in-situ HPGe  $\gamma$  spectrometers used for non-destructive analyzing radioactivity in nuclear facilities decommissioning, is presented. A series of assay for some stainless steel pipes and tanks in some nuclear facilities/laboratories of CIAE are taken on site with the in-situ HPGe  $\gamma$  spectrometer. At the same time, some examples are taken and analyzed in laboratories. The relative bias/variation between the values of activity measured by in-situ HPGe  $\gamma$  spectrometers on site and that analyzed in laboratory is less than  $\pm 45.0\%$ .

**Key words:** Calibration, MCNP, In-situ HPGe  $\gamma$  spectrometer, Decommissioning

## INTRODUCTION

Some nuclear facilities, such as old research reactors and nuclear fuel cycle installations, are candidates for near-term decommissioning in parallel with progressive ageing and technical-economical obsolescence. The success of a decommissioning project depends to a large extent on the adequacy of establishing the radiological inventory, covering radiation sources, contamination and activation products such as  $^{60}\text{Co}$  in structural steel. This process above is called radiological characterization. Radiological characterization will provide information important in order to identify contaminated/activated areas, delineate radiological controlled zones, estimate types, quantities and class of radioactive waste and to support planning and cost estimates<sup>[1,2]</sup>.

Non-Destructive Analysis (NDA) is one of the important techniques to determine radio-nuclides and radio-activities in radiological characterization survey of nuclear facilities decommissioning. The development of in-situ gamma spectrometers, which is one kind of NDA device, over the last decade has transformed this technique once confined to laboratories into a standard technique particularly suitable for building surfaces and soil measurements, and then contamination object measurements. A number of devices with Ge detectors are available, some of which have been specifically designed for clearance measurements of buildings and sites, using a collimator (thus restricting the area to be measured in order to allow quantitative measurements in  $\text{Bq}/\text{cm}^2$ ). These types of detectors require extensive calibration techniques. A new calibration technique, Monte Carlo calibration technique of HPGe spectrometers used for non-destructive analyzing radioactivity in nuclear facilities decommissioning, is presented in this paper<sup>[3]</sup>. And this technique was verified by some surveys of contamination sources on site of nuclear facilities and in laboratory of CIAE.

## 1 METHODS AND PRINCIPLES OF CALIBRATION

The principle of Monte Carlo method consists in simulating the history of a great number of the individual photon passing through the HPGe crystal. Physical quantities that obey statistical distribution are sampled according to the given distribution function.

Various steps in the history of a gamma-ray before it is completely absorbed or escapes are simulated by Monte Carlo process

### 1.1 The Mathematical Model for Calibrating Factors of a in-situ HPGe $\gamma$ Spectrometer

#### 1.1.1 Records

In order to obtain the calibration factors for the HPGe  $\gamma$  detector measuring radio-sources or radio-contaminants, the numbers of photon incidence into the Ge crystal, in which the energy of photon is completely deposited, are recorded.

If the energy ( $E$ ) of a photon is completely depleted in Ge crystal, one count is recor-

ded in the channel versus  $E$ , the total counts  $C_T$  in the channel versus  $E$  is,

$$C_T = \sum_m 1 \quad (1)$$

Because the skill of bias sampling for the direction of photons is used, the total counts  $C_T$  in the channel versus  $E$  is,

$$C_T = \sum_m f_m \quad (2)$$

Where,  $f_m$  is the rectifying a deviation factor for the  $m$ th photon whose energy is completely depleted in Ge crystal.

The number of photons sampled from radio-sources or radio-contaminants— $N$  must be recorded at the same time.

### 1.1.2 The physical quantities

The physical quantities to be obtained are the calibration factors  $\epsilon(E)$  for the HPGe  $\gamma$  detector vs radio-sources or objects contaminated. They can be calculated by formula (3):

$$\epsilon(E) = C_T/N \quad (3)$$

where,  $C_T$  is the tally in the channel of full energy peak.  $N$  is the number of photons sampled from radio-sources or radio-contaminants in MC modeling.

The calibration factor  $\epsilon(E)$  is related not only to geometrical parameters of the detector, but also to geometrical parameters and material of the collimator, geometrical parameters and material of the object measured, the distance from the detector to the object measured, and so on.

## 1.2 MC Modeling Code

The Monte Carlo modeling code—MCNP 4B was used to model calibration factors of the HPGe detector. The code is a large and multifunctional code system of particle transportation, which developed by the University of California at Los Alamos National Laboratory and used to compute the transportation of neutron, photon, electron or coupled neutron-photon-electron in any complicated geometry system. The coherent and non-coherent scattering photons are taken into account for photon. The possible fluorescence emitted and doublet produced after photoelectric adsorption are also disposed<sup>[4]</sup>.

The main contents of the input document include cell card, curved face card, mode card, cell parameter card, source feature card, tally card, material card and so on. The units of physical quantities inputted are following: Length(cm), Energy (MeV), Time( $10^{-8}$  s), Atomic density ( $10^{24}$  atom/cm<sup>3</sup>), mass density (mg/cm<sup>3</sup>), Cross-section (bar( $10^{-24}$  cm<sup>2</sup>)).

There are 8 output parameters of code MCNP-4B. Only output parameter F8 was used for tally of energy distribution of pulses created in a detector Charge deposition.

## 2 APPARATUS

The apparatus used by us is ISOCS—a  $\gamma$  spectrometer system, which is made by CANBERRA Co., USA. It consists of a HPGe  $\gamma$  detector, a multi-channel analyzer, a set of lead collimators, an AV-DV adapter and a cart, showed in Fig. 1.

## 2.1 Detector

The detector is N type HPGe  $\gamma$  detector. The geometric size of Ge crystal is  $\phi 70 \text{ mm} \times 30 \text{ mm}$ . The distance from the crystal surface to carbon window is 5 mm. The relative detection efficiency is 34.1%. The energy resolution for 1332.5 keV of  $^{60}\text{Co}$  FWHM  $\leq 2.1 \text{ keV}$ . A portable cryostat (Model 7935SL-5) full with 7 L liquid nitrogen can meet the needs of work 3 days. The energy range is 3 keV~3 MeV.

## 2.2 Multi-channel Analyzer

The multi-channel pulse analyzer is also made by CANBERRA Co., USA. It's a InSpector 2000 portable multi-channel pulse analyzer, whose size is 3.8 cm  $\times$  18.5 cm  $\times$  17.3 cm, weight is 1.3 kg (including battery).

## 2.3 Collimators

There are 8 parts of collimator, including 2.5 cm lead shielding on sides (3 parts), 2.5 cm lead end collimators with 90 deg and 30 deg hole, 5 cm lead shielding on sides, (3 parts),.

## 2.4 Wheeled Transport Cart

A wheeled cart assembly is used for easy transport. It includes 2 large wheels of 40 cm (16 in) in black, 2 small wheels of 20 cm (8 in) in front (rear wheels have individual locking brakes), a carrying tray for shields and an instrument shelf for MCA and PC.

# 3 GEOMETRICAL SIZE OF DETECTOR

Accurate geometrical parameters and material components are one of the key to obtain the calibration factors for HPGe  $\gamma$  detectors, when MC modeling is used. It is very pity that we often don't know the geometrical sizes and components of materials of the detector very well in detail. Some manufacturers of HPGe  $\gamma$  detector refuse to tell the details of the geometrical sizes and components of materials, except for the geometrical sizes of Ge crystal, by reason of commercial secret. It is also pity that the data of geometrical sizes given by some manufacturers are often neither complete nor accurate.

An experimental method of point sources combined with MC modeling techniques are used for determining the equivalent geometrical parameters of the HPGe  $\gamma$  detector. First, the original geometrical size of the detector can be obtained, according to the knowledge of HPGe  $\gamma$  detector, some parameters are given by manufacturers. Then, the detection effi-

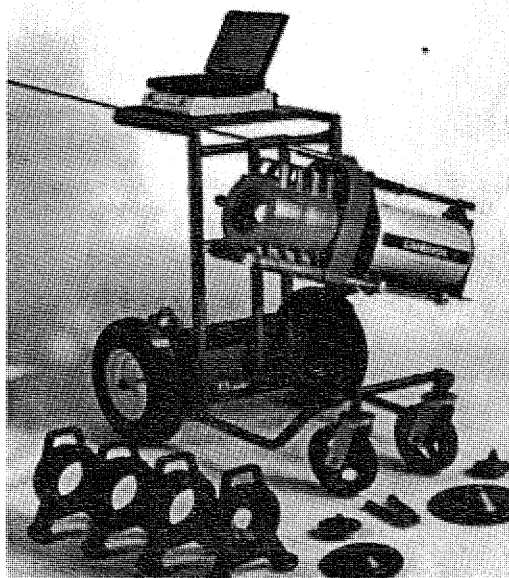


Fig. 1 The apparatus

ciencies based on the original geometrical size are modeled and compared with that of experiment. If the difference between them is not meet the need of error, fine modification is made for the geometrical size of the detector, then the detection efficiencies based on the new geometrical size are modeled and compared with that of experiment again, and so on. Not until the difference of the detection efficiencies between that modeled and experimented meet the need of error, do it stop modeling and comparing. Equivalent geometrical size of the detector is then determined.

### 3.1 Construction

The construction of HPGe  $\gamma$  detector is preliminarily determined according to the knowledge of HPGe  $\gamma$  detector made by CABBERRA Co.

and other manufactory, which shown in Fig. 2.

### 3.2 Radio-sources

Radio-sources used in the experiment are  $^{137}\text{Cs}$ ,  $^{60}\text{Co}$  and  $^{152}\text{Eu}$ , which are spot sources, with the diameter of radio-source spot is  $\phi < 5$  mm. The activities of them are from  $3.3 \times 10^5$  Bq to  $1.7 \times 10^6$  Bq.

### 3.3 MC Modeling and Experiment Verifying of Relative Detection Efficiency

The relative detection efficiency is one of the important parameters of HPGe  $\gamma$  detector. It is obtained by formula (4).

$$\epsilon(1\ 332.5\ \text{keV}) = \left( \frac{n}{A \times \eta} \right) / \delta \quad (4)$$

where,  $A$ —activity of  $^{60}\text{Co}$  point radio-source, Bq;

$\eta$ —emitting rate of photon with energy 1 332.5 keV;

$n$ —peak counting rate of energy  $E_\gamma$ ,  $\text{s}^{-1}$ . The distance from source to detector is 25 cm;

$\delta$ —absolute detection efficiency of 3 in $\times$ 3 in NaI(Tl) crystal,  $\delta = 1.2 \times 10^{-3}$ .

The relative detection efficiency in formula (4) was computed by MC modeling. The bias sampling technique with assistant ball circumscribing the detector are used in the MC modeling. Both modeling results and the experimental result are shown in Figure 3. In the former technique, partial sampling of incident direction of the un-collided photon from the point gamma sources with respect to the assisting circumscribed ball is used. The numbers of un-collided photon sampled from the point gamma sources must only be 200 000, if the statistic error less than 1% for the relative detection efficiency of 1 333 keV. 25 million of

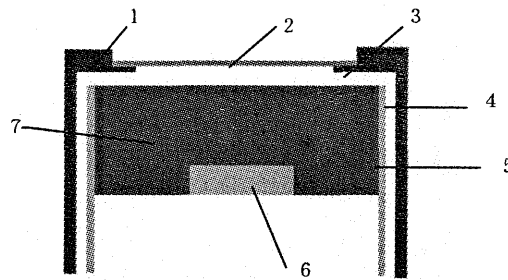


Fig. 2 Schematic diagram of construction for the HPGe  $\gamma$  detector

- 1—Aluminum shell; 2—Carbon window;
- 3—Support for carbon window; 4—Copper holder;
- 5—Ge dead layer; 6—Cooling finger hole; 7—Ge Crystal

the un-collided photon from the point gamma sources must sampled if the same statistic error and the bias sampling technique with assistant ball circumscribing the detector is not used.

### 3.4 The MC modeling and experimental validating of detection efficiency for HPGe $\gamma$ spectrometer vs point sources with different energy

In order to obtain and valid ate the “precise” geometrical sizes of the detector, following experiments are made. In those experiments, the same point radio-sources as listed in Table 1 are used and are respectively put at the locations which are different angles  $\theta$  with the axis of the detector, such as  $\theta=0^\circ, 15^\circ, 30^\circ, 45^\circ, 60^\circ, 75^\circ, 90^\circ$ . The distance of point source-detector is 1 m, shown in Fig. 4. Then the experimental values of detection efficiency for the point sources above are made.

Utilizing the primary geometrical sizes of HPGe detector and MC code, one can obtained the modeling values of detection efficiency for point sources. If the limit of difference between detection efficiency values MC modeled and measured is not achieved, the primary geometrical sizes is adjusted, and new modeling values of detection efficiency for the point sources are obtained, and then comparison is made again until the limit of difference between them is achieved.

The final modeling values and experimental values are list in Table 1, which are agreement within  $\pm 5\%$ . The geometrical sizes in the final modeling as the “correct” sizes of the HPGe detector are list in Table 2.

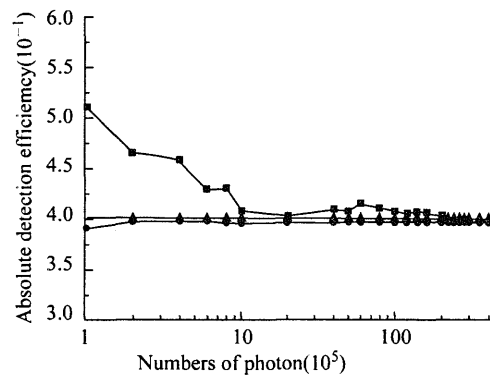


Fig. 3 Comparison of relative detection efficiency for a HPGe  $\gamma$  detector obtained by MC modeling and experiment measuring

■ direct sampling; ● bias sampling; ▲ experiment

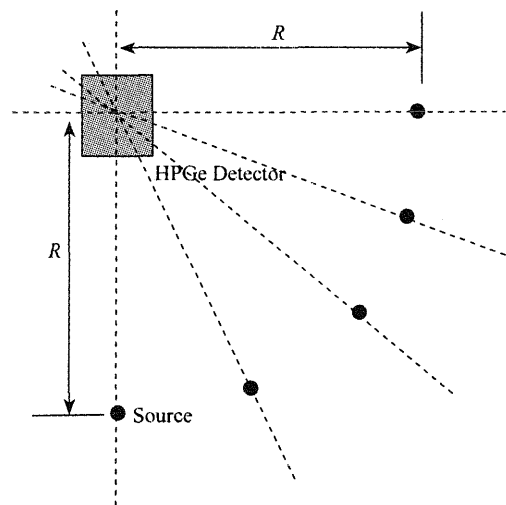


Fig. 4 Schematic diagram of relative location of point sources and the detector

**Table 1 Comparison of detection efficiency for a HPGe  $\gamma$  detector obtained by MC modeling and experiment measuring with no collimation**

Energy/ keV	121.8				244.7				344.3				661.7			
Angle $\theta(^{\circ})$	MC modeling	Exp. measuring	Relative error/%	MC modeling	Exp. measuring	Relative error/%	MC modeling	Exp. measuring	Relative error/%	MC modeling	Exp. measuring	Relative error/%	MC modeling	Exp. measuring	Relative error/%	
0	$2.78 \times 10^{-4}$	$2.85 \times 10^{-4}$	-2.46	$1.71 \times 10^{-4}$	$1.72 \times 10^{-4}$	-0.58	$1.18 \times 10^{-4}$	$1.21 \times 10^{-4}$	-2.48	$5.89 \times 10^{-5}$	$6.12 \times 10^{-5}$	-3.76	$5.89 \times 10^{-5}$	$6.12 \times 10^{-5}$	-3.76	
15	$2.73 \times 10^{-4}$	$2.77 \times 10^{-4}$	-1.44	$1.68 \times 10^{-4}$	$1.70 \times 10^{-4}$	-1.18	$1.14 \times 10^{-4}$	$1.19 \times 10^{-4}$	-4.20	$5.69 \times 10^{-5}$	$6.06 \times 10^{-5}$	-6.11	$5.69 \times 10^{-5}$	$6.06 \times 10^{-5}$	-6.11	
30	$2.53 \times 10^{-4}$	$2.53 \times 10^{-4}$	0	$1.63 \times 10^{-4}$	$1.59 \times 10^{-4}$	2.52	$1.15 \times 10^{-4}$	$1.13 \times 10^{-4}$	1.77	$5.82 \times 10^{-5}$	$5.78 \times 10^{-5}$	0.69	$5.82 \times 10^{-5}$	$5.78 \times 10^{-5}$	0.69	
45	$2.19 \times 10^{-4}$	$2.19 \times 10^{-4}$	0	$1.42 \times 10^{-4}$	$1.41 \times 10^{-4}$	0.71	$1.02 \times 10^{-4}$	$1.02 \times 10^{-4}$	0	$5.27 \times 10^{-5}$	$5.38 \times 10^{-5}$	-2.04	$5.27 \times 10^{-5}$	$5.38 \times 10^{-5}$	-2.04	
60	$1.75 \times 10^{-4}$	$1.69 \times 10^{-4}$	3.43	$9.30 \times 10^{-5}$	$1.14 \times 10^{-4}$	5.17	$6.97 \times 10^{-5}$	$8.53 \times 10^{-5}$	2.46	$4.86 \times 10^{-5}$	$4.80 \times 10^{-5}$	1.31	$4.86 \times 10^{-5}$	$4.80 \times 10^{-5}$	1.31	
75	$1.20 \times 10^{-4}$	$1.21 \times 10^{-4}$	-0.83	$7.60 \times 10^{-5}$	$9.25 \times 10^{-5}$	0.54	$5.88 \times 10^{-5}$	$7.06 \times 10^{-5}$	-1.27	$3.99 \times 10^{-5}$	$4.14 \times 10^{-5}$	-3.62	$3.99 \times 10^{-5}$	$4.14 \times 10^{-5}$	-3.62	
90	$7.99 \times 10^{-5}$	$8.20 \times 10^{-5}$	-2.56	$1.71 \times 10^{-4}$	$7.69 \times 10^{-5}$	-1.17	$1.18 \times 10^{-4}$	$6.15 \times 10^{-5}$	-4.39	$3.48 \times 10^{-5}$	$3.68 \times 10^{-5}$	-5.43	$3.48 \times 10^{-5}$	$3.68 \times 10^{-5}$	-5.43	
Energy/ keV	964.1				1173.2				1332.5				1408.0			
Angle $\theta(^{\circ})$	MC modeling	Exp. measuring	Relative error/%	MC modeling	Exp. measuring	Relative error/%	MC modeling	Exp. measuring	Relative error/%	MC modeling	Exp. measuring	Relative error/%	MC modeling	Exp. measuring	Relative error/%	
0	$4.08 \times 10^{-5}$	$4.30 \times 10^{-5}$	-5.12	$3.36 \times 10^{-5}$	$3.47 \times 10^{-5}$	-3.17	$2.97 \times 10^{-5}$	$3.08 \times 10^{-5}$	-3.57	$2.85 \times 10^{-5}$	$3.07 \times 10^{-5}$	-7.17	$2.85 \times 10^{-5}$	$3.07 \times 10^{-5}$	-7.17	
15	$3.98 \times 10^{-5}$	$4.23 \times 10^{-5}$	-5.91	$3.31 \times 10^{-5}$	$3.42 \times 10^{-5}$	-3.22	$2.95 \times 10^{-5}$	$3.04 \times 10^{-5}$	-2.96	$2.80 \times 10^{-5}$	$3.04 \times 10^{-5}$	-7.89	$2.80 \times 10^{-5}$	$3.04 \times 10^{-5}$	-7.89	
30	$4.17 \times 10^{-5}$	$4.08 \times 10^{-5}$	2.21	$3.49 \times 10^{-5}$	$3.31 \times 10^{-5}$	5.44	$3.07 \times 10^{-5}$	$2.95 \times 10^{-5}$	4.07	$2.95 \times 10^{-5}$	$2.94 \times 10^{-5}$	0.34	$2.95 \times 10^{-5}$	$2.94 \times 10^{-5}$	0.34	
45	$3.75 \times 10^{-5}$	$3.85 \times 10^{-5}$	-2.60	$3.15 \times 10^{-5}$	$3.11 \times 10^{-5}$	1.29	$2.82 \times 10^{-5}$	$2.78 \times 10^{-5}$	1.44	$2.69 \times 10^{-5}$	$2.82 \times 10^{-5}$	-4.61	$2.69 \times 10^{-5}$	$2.82 \times 10^{-5}$	-4.61	
60	$3.50 \times 10^{-5}$	$3.51 \times 10^{-5}$	-0.28	$2.90 \times 10^{-5}$	$2.81 \times 10^{-5}$	3.20	$2.63 \times 10^{-5}$	$2.53 \times 10^{-5}$	3.95	$2.66 \times 10^{-5}$	$2.56 \times 10^{-5}$	3.91	$2.66 \times 10^{-5}$	$2.56 \times 10^{-5}$	3.91	
75	$2.94 \times 10^{-5}$	$2.98 \times 10^{-5}$	-1.34	$2.52 \times 10^{-5}$	$2.51 \times 10^{-5}$	0.40	$2.25 \times 10^{-5}$	$2.26 \times 10^{-5}$	0.44	$2.16 \times 10^{-5}$	$2.30 \times 10^{-5}$	-6.09	$2.16 \times 10^{-5}$	$2.30 \times 10^{-5}$	-6.09	
90	$2.62 \times 10^{-5}$	$2.71 \times 10^{-5}$	-3.32	$2.30 \times 10^{-5}$	$2.33 \times 10^{-5}$	-1.29	$2.07 \times 10^{-5}$	$2.12 \times 10^{-5}$	-2.36	$1.98 \times 10^{-5}$	$2.14 \times 10^{-5}$	-7.48	$1.98 \times 10^{-5}$	$2.14 \times 10^{-5}$	-7.48	



**Table2 Geometric sizes of the HPGe detector**

No.	Item	Size/cm
1	Ge Crystal (Diameter×Length)	φ6.86×2.97
2	Thickness of Ge insensitive layer	0.01
3	Thickness of copper holder	0.244
4	Cooling finger hole (Diameter×Length)	φ2.0×0.188
5	Thickness of aluminum shell (Diameter×Length)	φ8.89×0.2
6	Thickness of carbon window	0.5
7	Thickness of Al support for carbon window	0.16
8	Distance from surface of crystal to the window	0.545

### 3.5 Verification of the parameters for collimator

The material and geometrical sizes of collimator are also important parameters used for MC modeling calibration factors of in-situ spectrometer. One can verify the accuracy of the parameters of collimator by comparing the shielding effect of MC modeling with that of experiment.

The same point sources are located at the same location as chapter 4. 4, shown in Fig. 5. The detection efficiencies of MC modeled and experimental measured. The detection efficiencies of MC modeled and experimental measured for 3 radio-sources (there are 8 energies) and 4 locations ( $\theta=0^\circ, 30^\circ, 60^\circ$  and  $90^\circ$ ) are shown in Fig. 6. They are agreement within  $\pm 35\%$ .

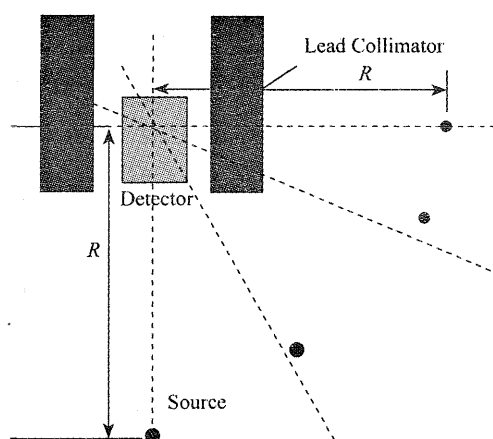


Fig. 5 Schematic diagram of relative location of radio-sources and the detector with lead collimator

## 4 MEASUREMENT AND VALIDATION IN LABORATORY AND SITE

### 4.1 Establishment of the Techniques

With the “accurate” geometrical sizes of the HPGe detector and collimator, the calibration factors  $\epsilon(E)$  of various contamination objects in nuclear facilities decommissioning are obtained by MCNP. When the in-situ HPGe  $\gamma$  spectrometer is used for measuring various contamination objects in nuclear facilities decommissioning, the radio-activities in/on those contamination objects can be obtained.

## 4.2 Calibration Factors and Experimental Validation

In order to validate the adaptability of in-situ measurement technique for the HPGe  $\gamma$  spectrometer, a series of experimental validation are made for radio-nuclides in some objects at different site, such as in model pieces at laboratory and contamination objects at some nuclear facilities.

### 4.2.1 Calibration factors and experimental validation of model pieces in laboratory

#### 4.2.1.1 Calibration factors and experimental validation of pipe model pieces contaminated

##### (1) Radioactive area source

Five sheets of radioactive area source, 2 sheet for  $^{137}\text{Cs}$ , 2 sheet for  $^{60}\text{Co}$  and 1 sheet for  $^{241}\text{Am}$ , are prepared. The sizes, area, activity and mean activity of radioactive area source are shown in Table 3. The uncertainty of sources is less than 5% ( $k=1$ ).

##### (2) Preparation of stainless steel pipe piece with radio-contamination

Some stainless steel pipes with different diameter are made, shown in Fig. 7. The geometrical sizes of the pipe are 61~

113 mm for external diameter, 56.0~103 mm for internal diameter, 2.26~5 mm for wall thickness and 255 mm for length. The area sources are rolled into cylinder and inserted into the pipes or covered on the surface of the pipe respectively, modeling the cases of internal/external contamination of stainless steel pipes. More pipes with different wall thickness are obtained by inserting some litter pipe into a large pipe.

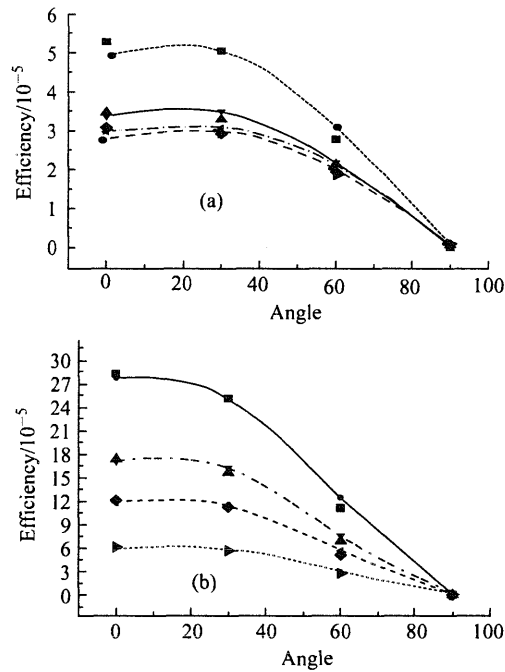


Fig. 6 Comparison of detection efficiency values obtained by MC modeling and experiment for the detector with collimator

- (a) Energy(keV)
- 778.9 experiment value;
  - 778.9 emulation value;
  - ▲ 1 173 experiment value;
  - ▼ 1 173 emulation value;
  - ◆ 1 332 experiment value;
  - ◄ 1 332 emulation value;
  - 1 408 experiment value;
  - 1 408 emulation value
- (b) Energy(keV)
- 121.8 experiment value;
  - 121.8 emulation value;
  - ▲ 244.7 experiment value;
  - ▼ 244.7 emulation value;
  - ◆ 344.3 experiment value;
  - ◄ 344.3 emulation value;
  - 661.7 experiment value;
  - 661.7 emulation value

Table 3 The basic parameters of area sources  $^{137}\text{Cs}$ ,  $^{60}\text{Co}$  and  $^{241}\text{Am}$  prepared

No	Radio-nuclide	Size of Area/cm	Area/cm <sup>2</sup>	Activity/10 <sup>4</sup> Bq	Mean activity/(Bq/cm <sup>2</sup> )
1	$^{137}\text{Cs}$	21×28	588	6.714	1.142×10 <sup>2</sup>
2	$^{137}\text{Cs}$	23×23	529	6.854	1.296×10 <sup>2</sup>
3	$^{60}\text{Co}$	21×28	588	7.622	1.296×10 <sup>2</sup>
4	$^{60}\text{Co}$	23×23	529	7.781	1.471×10 <sup>2</sup>
5	$^{241}\text{Am}$	21×28	588	3.617	6.151×10

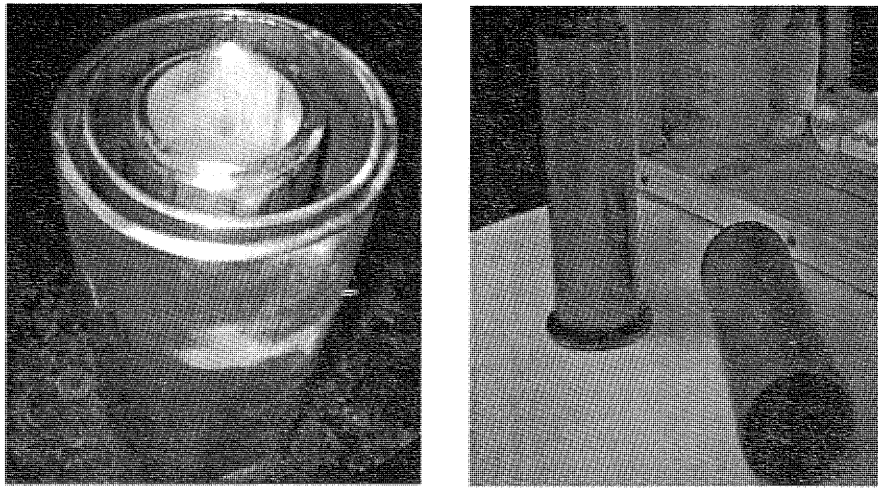


Fig. 7 The stainless steel pipe used as modeling pieces of external/internal surface contamination

### (3) Measurement of stainless steel pipe piece contaminated

A collimator was made with 4 lead shields. The distance from the geometrical center of HPGe  $\gamma$  detector to the axis of stainless steel pipe piece is 81.8 cm.

The count rates (CPS) of the full energy peak were obtained by measurement. The calibration factors (CPS/(Bq/cm<sup>2</sup>) or CPS/(Bq/kg)) were obtained by modeling code MCNP 4B with input of relative parameters of the detector and the contamination object measured. The radio-activities (Bq/cm<sup>2</sup> or Bq/kg) on/in the contamination object measured could be obtained.

### (4) Results and Comparison

Both the rating and measuring values of contamination radio-nuclides in stainless steel pipe with different diameters of pipe and thickness of wall are listed in Table 4. They are agreement within  $\pm 7.5\%$ , and average relative error is  $-1.31\%$ .

#### 4.2.1.2 Experimental validation for measuring large contamination pieces

In order to validate the adaptability of the in-situ HPGe  $\gamma$  spectrometer measuring large contamination model pieces, one large volume source in the Aerial Survey and Remote Sensing Center of China National Nuclear Corporation (CNNC) was selected as the object measured by the in-situ HPGe  $\gamma$  spectrometer.

##### (1) Introduction of the large volume source

There are 13 large volume sources (LVS) established by the Aerial Survey and Remote Sensing Center of CNNC. They are located at a wide lawn with distance of 25 m from each other, shown in Fig. 8. The geometrical size of every LVS is  $\phi 2.2 \text{ m} \times 0.6 \text{ m}$ . They were made by mixing concrete, quartz sand with powder of Uranium-Radium, Thorium or K respectively. The density and the components of every large volume sources can be seen in reference[5].

Table 4 Comparison of NDA values and rating values of radio-activity in modeling pieces of stainless steel pipe contaminated

Cont. Isot.	Energy/ keV	Conta. Location	Exit bit of the pipe/cm	Wall thickness/cm	Count rate of full peak/cps	Calibration Factor (MC)/(10 <sup>-2</sup> cps/(Bq/cm <sup>2</sup> ))	Area Activity (measured)/(Bq/cm <sup>2</sup> )	Area Activity (rating)/(Bq/cm <sup>2</sup> )	Relative Bias/%
<sup>241</sup> Am	59.5	External surface	8.71	0.226	3.069	4.68	6.558×10	6.151×10	6.62
			8.71	0.582	2.935	4.66	6.298×10	6.151×10	2.39
		8.71	1.282	2.921	4.66	6.298×10	6.151×10	2.39	
				2.929	4.66	6.298×10	6.151×10	2.39	
<sup>137</sup> Cs	661.67	External surface	8.71	0.226	3.977	3.60	1.105×10 <sup>2</sup>	1.142×10 <sup>2</sup>	-3.24
			8.71	0.582	3.447	3.16	1.091×10 <sup>2</sup>	1.142×10 <sup>2</sup>	-4.47
		8.71	1.282	3.260	2.87	1.136×10 <sup>2</sup>	1.142×10 <sup>2</sup>	-0.53	
				3.163	2.76	1.146×10 <sup>2</sup>	1.142×10 <sup>2</sup>	0.35	
<sup>137</sup> Cs	661.67	Internal surface	8.06	0.356	3.431	2.72	1.261×10 <sup>2</sup>	1.296×10 <sup>2</sup>	-2.70
			8.51	0.582	2.954	2.32	1.273×10 <sup>2</sup>	1.296×10 <sup>2</sup>	-1.77
		9.51	1.082	2.481	1.92	1.292×10 <sup>2</sup>	1.296×10 <sup>2</sup>	-0.31	
				2.249	1.65	1.363×10 <sup>2</sup>	1.296×10 <sup>2</sup>	5.17	
<sup>60</sup> Co	1173.2	External surface	10.11	1.382	1.852	1.33	1.392×10 <sup>2</sup>	1.296×10 <sup>2</sup>	7.41
			8.71	0.226	3.148	2.54	1.239×10 <sup>2</sup>	1.296×10 <sup>2</sup>	-4.40
		8.71	0.98	2.776	2.29	1.212×10 <sup>2</sup>	1.296×10 <sup>2</sup>	-6.48	
				2.549	2.08	1.225×10 <sup>2</sup>	1.296×10 <sup>2</sup>	-5.48	
8.71	1.28	2.366	2.00	1.183×10 <sup>2</sup>	1.296×10 <sup>2</sup>	-5.94			

Continue

Cont. Isot.	Energy/ keV	Conta. Location	Ex bit of the pipe/cm	Wall thickness/cm	Count rate of full peak/cps	Calibration Factor (MC)/(10 <sup>-2</sup> cps/(Bq/cm <sup>2</sup> ))	Area Activity (measured)/(Bq/cm <sup>2</sup> )	Area Activity (rating)/(Bq/cm <sup>2</sup> )	Relative Bias/%
<sup>60</sup> Co	1 173.2	Internal	8.06	0.36	2.956	2.00	1.478×10 <sup>2</sup>	1.471×10 <sup>2</sup>	0.48
			8.51	0.58	2.616	1.71	1.530×10 <sup>2</sup>	1.471×10 <sup>2</sup>	4.01
		surface	9.11	0.88	2.244	1.54	1.457×10 <sup>2</sup>	1.471×10 <sup>2</sup>	-0.95
			9.51	1.08	2.033	1.38	1.473×10 <sup>2</sup>	1.471×10 <sup>2</sup>	0.14
			10.11	1.38	1.758	1.18	1.471×10 <sup>2</sup>	1.29	
<sup>60</sup> Co	1 332.5	Internal	8.06	0.36	2.657	1.81	1.468×10 <sup>2</sup>	1.471×10 <sup>2</sup>	-0.21
			8.51	0.58	2.361	1.58	1.494×10 <sup>2</sup>	1.471×10 <sup>2</sup>	1.56
		surface	9.11	0.88	2.056	1.47	1.399×10 <sup>2</sup>	1.471×10 <sup>2</sup>	-4.89
			9.51	1.08	1.862	1.34	1.390×10 <sup>2</sup>	1.471×10 <sup>2</sup>	-5.51
			10.11	1.38	1.635	1.16	1.471×10 <sup>2</sup>	-4.21	
<sup>60</sup> Co	1 332.5	External	8.71	0.23	2.815	2.28	1.235×10 <sup>2</sup>	1.296×10 <sup>2</sup>	-4.71
			8.71	0.58	2.512	2.05	1.225×10 <sup>2</sup>	1.296×10 <sup>2</sup>	-5.48
		surface	8.71	0.98	2.270	1.87	1.214×10 <sup>2</sup>	1.296×10 <sup>2</sup>	-6.33
			8.71	1.28	2.153	1.79	1.203×10 <sup>2</sup>	1.296×10 <sup>2</sup>	-7.18

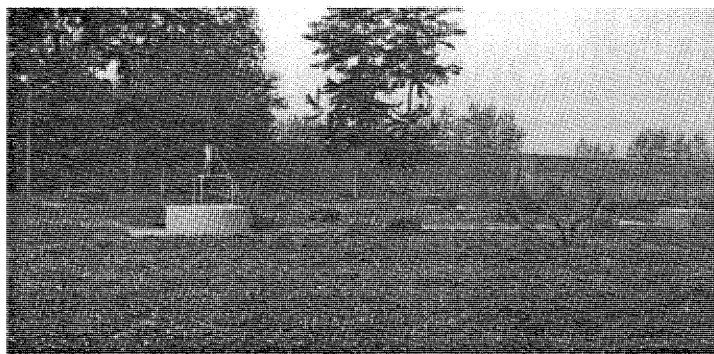


Fig. 8 Large volume sources in the Aerial Survey and Remote Sensing Center of CNNC

### (2) In-situ measurement

The collimator consists of 4 lead shields. The detector is on the top of the large volume source, shown in Fig. 8. The large volume source (MY3), in which the U-Ra, Th and K powder are mixed, was measured. The distance from detector to top surface of the source is 1 m.

### (3) Results and comparisons

The radioactive concentration is equal to the count rates of the full energy peak divided by the calibration factor of different energy, which was calculated by Monte Carlo modeling.

We obtained the average radioactive concentration of the series of  $^{238}\text{U}$ - $^{226}\text{Ra}$  and  $^{232}\text{Th}$ , using several radioactive concentration calculated by several  $\gamma$  energy from the daughters of the series of  $^{238}\text{U}$ - $^{226}\text{Ra}$  and  $^{232}\text{Th}$ . The comparison of measuring values and rating values of radio-activity in a standard large volume source—YM3 is shown in Table 5.

Table 5 Comparison of measuring values and rating values of radio-activity in a standard large volume source-YM3

Decay series	Radio-Nuclide	Energy/ MeV	Measuring value in site				Rating Activity/ ( $10^2\text{Bq/kg}$ )	Relative error/%
			Count rate/ $10^{-1}\text{s}^{-1}$	Cali. Factor/ ( $10^{-4}\text{cps}/(\text{Bq/kg})$ )	Activity/ ( $10^2\text{Bq/kg}$ )	Average/ ( $10^2\text{Bq/kg}$ )		
$^{238}\text{U}$ - $^{226}\text{Ra}$	$^{214}\text{Bi}$	0.609 3	5.14	8.32	6.18	6.88	-8.75	
	$^{214}\text{Bi}$	1.120 3	1.61	2.37	6.80			
$^{232}\text{Th}$	$^{214}\text{Bi}$	1.764 5	1.53	2.00	7.65	5.85	7.93	
	$^{228}\text{Ac}$	0.338 7	1.51	3.00	5.03			
	$^{214}\text{Ac}$	0.911 2	2.50	4.38	5.71			
	$^{228}\text{Ac}$	0.968 8	1.40	2.64	5.30			
	$^{208}\text{Pb}$	2.614 5	2.79	3.80	7.35			

#### 4.2.2 Verification of in-situ measurement in nuclear facilities with contaminated objects

Two pieces of contaminated object in different nuclear facilities were chosen to verify

this apparatus's quantitative analysis capability. One is a dissolved pot made by stainless steel, in which a bar of spent fuel was dissolved, and the other is a piece of stainless steel pipe used in the low-radioactivity liquid waste processing workshop (106#), in CIAE.

#### 4.2.2.1 Experimental verification of the internal surface contamination of dissolved pot

##### (1) In-situ measurement

An in-situ measurement was made to obtain the "background" spectrum for the spent fuel dissolved pot, before the spent fuel was dissolved. After a bar of spent fuel was dissolved in the pot, an in-situ measurement was made again when the dissolved liquid was vented. The dose rate was 200 nGy/h at the location of the detector, which was about twice of the background level.

The collimator consists of 4 lead shields. The distance was 14.1 cm from surface of the detector to the dissolved pot, shown in Fig. 9. The in-situ measurements from 2 directions were made because a few pipes inserted not symmetrically in the dissolved pot.

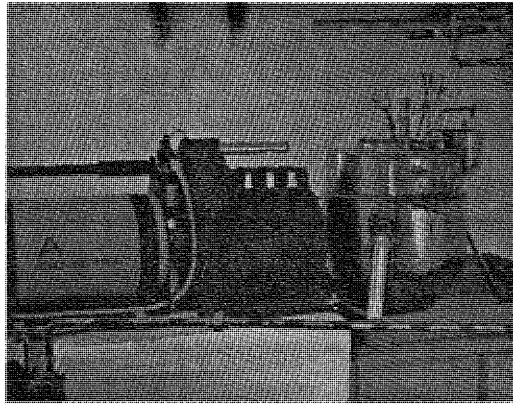


Fig. 9 In-situ measurement of the internal surface contamination of the spent fuel dissolved pot

##### (2) Sample analysis

In order to compare with the in-situ measurement results, a steel sheet ( $3\text{ cm} \times 1\text{ cm} \times 0.02\text{ cm}$ ) which component is the same as the pot was hung in the 1/4 height of the dissolved pot from bottom and dipped in the same dissolved liquid. After the dissolved liquid was vented, the steel sheet was taken out and sent for laboratory analysis. The laboratory analysis was done by the Nuclear Safeguards Technology laboratory in CIAE.

##### (3) Results and Comparisons

The results of in-situ HPGe  $\gamma$  spectrometer measuring and sample analyzing were shown in table 6.

The significant difference can be seen for the radio-activities measured from different directions from table 6. But the average relative error of  $-10.46\%$  is still a good result for NDA analysis.

**Table 6 Comparison of in-situ measuring values and sample analyzing values of surface contamination on the internal wall of melting pot for spent fuel elements**

No	Radio. Nucli.	Count rate/ cps	Cal. Factor/ (cps/(Bq/cm <sup>2</sup> ))	NDA act. / (Bq/cm <sup>2</sup> )	Sample ct. / (Bq/cm <sup>2</sup> )	Relative error/%
1	<sup>137</sup> Cs	123.9	1.92	64.37		-3.93
2		93.5	1.68	55.62	67.0	-16.99
	Average	108.7	1.39	78.36		-10.46

#### 4.2.2.2 Experimental verification in contaminated pipes of low radioactive level liquid waste processing workshop

##### (1) In-situ measurement

This in-situ measurement of HPGe  $\gamma$  spectrometer was made in the low radioactive level Liquid Waste Processing Workshop (LWPW) in CIAE. The dose rates were between 300 nGy/h and 2 mGy/h in controlled zone. The dose rate was  $3.0 \times 10^4$  nGy/h at the measured position. The contamination object measured was a stainless steel pipe ( $\phi 56$  mm  $\times$  162 mm, 3 mm thickness). The distance was 32.9 cm between the HPGe incidence window surface and the axis of stainless steel pipe, shown in Fig. 10.

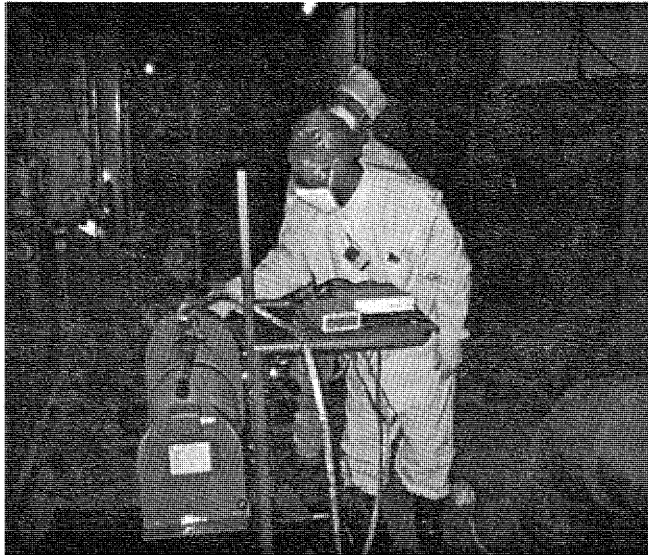


Fig. 10 In-situ measuring a radioactive contaminated stainless steel pipe in the controlled zone of 106# workshop

##### (2) Sample analysis in laboratory

The contaminated pipe was sampled by saw. The sample was dissolved by 6 mol/L hydrochloric acid (HCl) and sample solution was measured by the HPGe  $\gamma$  spectrometer with low-background in Health Physics division of CIAE.



### (3) Results and Comparisons

The NDA activities by the HPGe  $\gamma$  spectrometer and samples chemical analyzing activities in laboratory were shown in table 7.

**Table 7 Comparison of NDA and Sample analyzing values of surface contamination on the internal wall of steel pipe in 106 # workshop**

Rad. Nuc.	Count rate of full peak/s <sup>-1</sup>	Detection efficiency/ (cps/(Bq/cm <sup>2</sup> ))	NDA activity/ (Bq/cm <sup>2</sup> )	Average activity/ (Bq/cm <sup>2</sup> )	Sample activity/ (Bq/cm <sup>2</sup> )	Relative error/%
<sup>137</sup> Cs	108.42	$3.372 \times 10^{-5}$	$2559 \pm 256$	—	$2000 \pm 104$	28.1
	1.29 (1173 keV)	$3.44 \times 10^{-2}$	$37.5 \pm 3.71$	$32.5 \pm 2.30$	$12.6 \pm 0.3$	158
<sup>60</sup> Co	0.85 (1333 keV)	$3.10 \times 10$	$27.4 \pm 2.73$			

From table 7, we can see that, the NDA and sample analyzing values are agreement within 28% for <sup>137</sup>Cs, and within 158% for <sup>60</sup>Co.

There are three main causes for the difference of <sup>137</sup>Cs radioactivity obtained by the in-situ HPGe  $\gamma$  spectrometer and laboratory analysis; 1) some of <sup>137</sup>Cs was lost because of heating the immersed solution; 2) the contribution of ambient contaminated sources when in-situ measurement; 3) a larger error of geometrical size of object measured.

The relative error of surface radioactivity between the in situ measurement and the traditional laboratory analysis was 158%. The reasons maybe; 1) the penetrating coefficient of high energy photon (<sup>60</sup>Co) is higher, and 2) the radioactivity of <sup>60</sup>Co was too low, so it's statistic error of the full energy peak count rates was larger.

## 5 ERROR ANALYSIS OF THE NON—DESTRUCTIVE MEASUREMENT

### 5.1 The Subentry Analysis of Error

The main sources of the error in this technology are:

(1) The uncertainty of calibration factors by Monte Carlo calculation, Such as, the geometrical error between the calculation model and practical object, the statistical error contributed by the number of tracked particles in Monte Carlo modeling, the error contributed by the cross section data and density, and so on. The uncertainty of calibration factor by Monte Carlo modeling is less than  $\pm 5\%$ .

(2) The error of distance from the detector to the object measured. In generally, the distance between the detector and the object measured is great than and equal to 30 cm, so the relative error is less than  $\pm 6\%$ .

(3) The accurate geometrical condition can be obtained commonly by consulting original design drawings. But the error is less than  $\pm 4\%$  due to the eroding and abrading of

the metal materials.

(4) The statistical error of the full energy peak count rates is less than  $\pm 2\%$  for in-situ measurements.

(5) The error caused by the spectrum analysis is less than  $\pm 3\%$ .

(6) The error caused by the radiation field out of the "sight field" of the detector. If the dose rate at the location of the detector is 1 mGy/h, which produced by the same nuclide, like  $^{137}\text{Cs}$ ,  $^{60}\text{Co}$  et al, the relative error is less than  $\pm 20\%$ .

## 5.2 Total Uncertainty

The total uncertainty  $U$  is:

$$U = K \cdot \left[ \sum_i A_i^2 + 1/3 \sum_j B_j^2 \right]^{1/2} \quad (5)$$

Where  $A_i$  is the  $i$ th subentry in A sort;  $B_j$  is the  $j$ th subentry in B sort;  $K$  is the confidence coefficient.

The uncertainty of radioactivity measured by the HPGe  $\gamma$  spectrometer is less than 45% ( $K=3$ ) in this research.

## 6 CONCLUSIONS

(1) The radio-nuclides and their activities of contaminating object in decommissioning nuclear facilities are easily obtained with the in-situ measurement of HPGe  $\gamma$  spectrometer and calibration techniques.

(2) The advantage of MC modeling calibration factors is that the calibration factors of in-situ HPGe  $\gamma$  spectrometer can be easily obtained by only input of geometrical sizes and materials of object measured.

(3) The difference between radio-activity obtained by in-situ HPGe  $\gamma$  spectrometer and destructive samples analysis is less than 35%, under the radiation field of 30 000 nGy/h.

(4) The measuring technology of in situ  $\gamma$  spectrometer established in this research can be used in most conditions of decommissioning nuclear facilities, with the uncertainty of the radioactivity measured is  $< 45\%$  ( $K=3$ ).

### Reference

- 1 W. J. 曼尼拉, T. S. 拉瓜迪亚编. 张树璋, 郑福彰, 等译. 核设施退役手册. 北京: 原子能出版社, 1991
- 2 美国能源部主编. 美国 Enserch 环境公司编写. 王世盛, 薛维明, 陈德生, 等译. 核设施退役手册 (1994). DOE/EM-0142P, 北京: 核科学技术情报研究所, 1996. 8
- 3 A. Al-Ghamdi, X. G. Xu. Estimating the Depth of Embedded Contaminants from In-Situ Gamma Spectroscopic Measurements. Health Physics, 2003, 84(5): 632
- 4 邓力, 刘杰, 张文勇. 粒子输运蒙特卡罗程序 MCNP 在 MPI 下的并行化及完善. 数值计算与计算机应用, 2003, (3): 161~166
- 5 肖雪夫, 张积运, 马国学, 等. 环境电离模型辐射体源放射性核素活度浓度的 HPGe $\gamma$  谱仪就地测定. 辐射防护, 2003, 23(5): 278